Inband Scattering from Arrays with Series Feed Networks

David C. Jenn, *Senior Member, IEEE*, and Seunghoon Lee, *Senior Member, IEEE*

***Abstract*—Approximate equations are presented for the radar cross section (RCS) of a phased array antenna with a series feed beamforming network. The incident radar wave is assumed to be at the same frequency as the antenna operating frequency. In deriving the RCS formulas, multiple reflections are neglected, and like devices in the feed are assumed to have identical transmission and reflection coefficients. The approximate results are shown to be in excellent agreement with results obtained using a scattering matrix approach. The behavior of the RCS as a function of several feed design parameters is also investigated.**

I. Introduction

THE radar cross section (RCS) of a target not only depends on the physical shape and its composite materials, but also on its subcomponents such as antennas and other sensors. These components on the platforms may be designed to meet low RCS requirements as well as their sensor system requirements. In some cases, the onboard sensors can be the predominant factor in determining a platform's total RCS. A typical example is a reciprocal high gain antenna on a low RCS platform. If the antenna beam is pointed toward the radar and the radar frequency is in the antenna operating band, the antenna scattering can be significant.

Scattering from antennas has been the subject of interest since the 1950's. Extensive work has been done with regard to the determination of the antenna parameters [1], dipole scattering, and the effect of the terminal load impedance [2]. The RCS of horns [3], reflector antennas [4], and microstrip elements and arrays [5] have also been studied extensively. Detailed analysis of the inband scattering characteristics of arrays with parallel feed networks have been performed as well [6].

Another problem of interest is the scattering from phased arrays with series feed networks as shown in Fig. 1. A series feed is one in which the power to each element is tapped off of a main line sequentially. The coupling values are adjusted to provide the desired amplitude distribution. The most common method of terminating the main line is matched loading; another is to use a short, called a standing wave feed. For the loaded case, some power is always reflected from the load at the end of the main line which gives rise to a "reflection lobe" in the radiation pattern. It is reduced in magnitude relative to the main beam by an amount determined by the load reflection coefficient.

Manuscript received October 20, 1994; revised March 3, 1995.

D. C. Jenn is with the Naval Postgraduate School, Monterey, CA 93943 USA.

S. Lee is with the Republic of Korea Army.

IEEE Log Number 9412907.

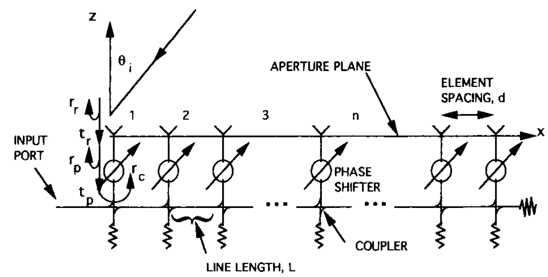

Fig. 1. Series feed antenna network.

For the inband RCS case, that is, where the antenna operates at the same frequency as the illuminating radar, the signal will penetrate into the feed and be reflected at the mismatches and junctions of the devices. This occurs even for an array with well-matched devices because of imperfections within the feed that cannot be avoided in the manufacturing and assembly processes. The total scattered power is a small fraction of the incident power, but for a large array, a large number of reflections can add constructively under some conditions yielding a large RCS.

High performance arrays must not only meet the system operating requirements (i.e., high gain, low sidelobe levels, etc.), but also the RCS requirements. To optimize the trade-offs between antenna RCS and radiation performance, an efficient and accurate model of RCS is crucial. This paper presents an approximate inband scattering model for arrays with series feeds. The approximate model is shown to be in good agreement with a more rigorous scattering matrix approach. The behavior of the RCS as a function of various array design parameters is also investigated.

II. Array Radar Cross Section

There are two antenna scattering modes to consider in the calculation of RCS [7]. The first is the antenna or radiation mode which is determined by the radiation properties of the antenna and vanishes when the antenna is conjugate matched to its radiation impedance. The second is the structural mode which is generated by the induced currents on the antenna surfaces. The approximate model only considers the antenna mode because it is a dominant RCS contribution for a free-standing phased array in its operating band, except possibly at wide angles where the array edge effects become important.

Total RCS can be computed by summing the scattering from all of the signals that enter the array, are reflected by the mismatches in the feed, and then return to the aperture. The

RCS is obtained by applying the basic equation of antenna scattering and summing over all of the array elements [6]. The monostatic RCS of a linear array of N identical elements is

$$\sigma(\theta,\phi) = \frac{4\pi A_e^2}{\lambda^2}\left|\sum_{n=1}^{N}\Gamma_n(\theta,\phi)e^{j\vec{k}\cdot\vec{d}_n}\right|^2 |F_{\rm norm}(\theta,\phi)|^2 \quad (1)$$

where

$\Gamma_n(\theta,\phi) =$ total reflected signal returned to the aperture for element n when the wave is incident from the (θ,ϕ) direction

$\vec{k} = k(u\hat{x}+v\hat{y}+w\hat{z}),\ k=2\pi/\lambda$

$u = \sin\theta\cos\phi$

$v = \sin\theta\sin\phi$

$w = \cos\theta$

$\vec{d}_n =$ position vector to element n

$A_e =$ effective area of an element

$F_{\rm norm} =$ normalized element scattering pattern.

Note that the assumption of identical elements in (1) neglects mutual coupling changes near the array edges.

There are two approaches to obtaining Γ_n in (1). The first is to use a network matrix method such as scattering parameters [8]. All interactions between the feed devices are included. The scattering matrix approach is computationally intense because a matrix equation must be solved. As N increases, the size of the matrix increases. A second approach is to trace signals through the feed. Tracing the signal flow inside a feed network, however, can be an extremely difficult and tedious job, especially if multiple reflections are included. For simplicity, the following approximations are made in the feed scattering model:

1) Devices of the same type are assumed to have identical electrical characteristics. For example, all of the radiating elements have the same reflection and transmission coefficients (denoted r_x and t_x, where $x = r, p, c$ for radiator, phase shifter, or coupler). The exception is the phase shifters which have a transmission coefficient of the form

$$t_{p_n} = t_p e^{j\chi_n}$$

where

$\chi_n = (n-1)\alpha_s,$

$\alpha_s = k\sin\theta_s\cos\phi_s = k\,d_x u_s,$

$(\theta_s,\phi_s) =$ the direction of the array radiation beam.

Thus the magnitude of the transmission coefficient is the same for all phase shifters ($|t_{p_n}| = t_p$), but the phase is allowed to vary linearly across the aperture.

2) The feed devices are well matched so that $r \ll 1$, and therefore higher order reflections can be neglected.

3) Lossless devices are assumed

$$|r|^2 + |t|^2 = 1.$$

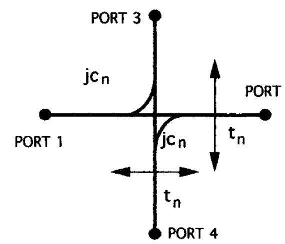

Fig. 2. Coupling and transmission paths for a four-port coupler.

With the previous assumptions and limitations, the fraction of the incident signal entering the array and returning to the aperture for reradiation is

$$\Gamma_n = r_r e^{j(n-1)\alpha} + t_r^2 r_p e^{j(n-1)\alpha} + t_r^2 t_p^2 r_c e^{j2(n-1)\alpha_s} \cdot e^{j(n-1)\alpha} + t_r^2 t_p^2 e^{j(n-1)\alpha_s} E_n \quad (2)$$

where $\alpha = k\,d_x u$ is the incident wave inter-element space delay. (Element 1 is used as a phase reference.) E_n represents the signal re-emerging from the series feed at element n. Some of this signal is due to reception from elements toward the input $(m < n)$, some is due to reception from elements toward the termination $(m > n)$, and some is due to reflection at the load at coupler n.

Equation (2) shows that the total scattered field is a sum of scattered fields from each group of devices in the feed

$$|E^s| = |E_r^s + E_p^s + E_c^s + E_s^s|. \quad (3)$$

E_s^s is the total scattered field due to the series feed reflections and is obtained by summing over all E_n as described in the next section. Assuming that only one component dominates at any given angle, it is sufficient to approximate the magnitude squared of the sum in (3) by the sum of the magnitudes squared

$$|E^s|^2 \approx |E_r^s|^2 + |E_p^s|^2 + |E_c^s|^2 + |E_s^s|^2. \quad (4)$$

Inserting (2) into (1) yields the RCS of the array. Because of the assumptions made with regard to the device scattering properties, it is possible to reduce some of the terms in (1) to closed form. The terms in (2) with factors r_r, r_p, and r_c can be summed to obtain

$$\sigma_r \approx \frac{4\pi A^2\cos^2\theta}{\lambda^2} r_r^2 \left[\frac{\sin(N\alpha)}{N\sin(\alpha)}\right]^2 \quad (5)$$

$$\sigma_p \approx \frac{4\pi A^2\cos^2\theta}{\lambda^2} r_p^2 t_r^4 \left[\frac{\sin(N\alpha)}{N\sin(\alpha)}\right]^2 \quad (6)$$

$$\sigma_c \approx \frac{4\pi A^2\cos^2\theta}{\lambda^2} r_c^2 t_r^4 t_p^4 \left[\frac{\sin(N\zeta)}{N\sin(\zeta)}\right]^2 \quad (7)$$

where $\zeta = \alpha + \alpha_s$. The total effective area of the array is $A \approx NA_e \approx N\ell d$ where ℓ is the effective length of the aperture element in the plane transverse to the array axis.

III. Derivation of the Series Feed RCS Formulas

Fig. 2 shows the signal distribution for the nth four port coupler with coupling coefficient c_n and transmission coefficient t_n. To begin with, the couplers are assumed lossless,

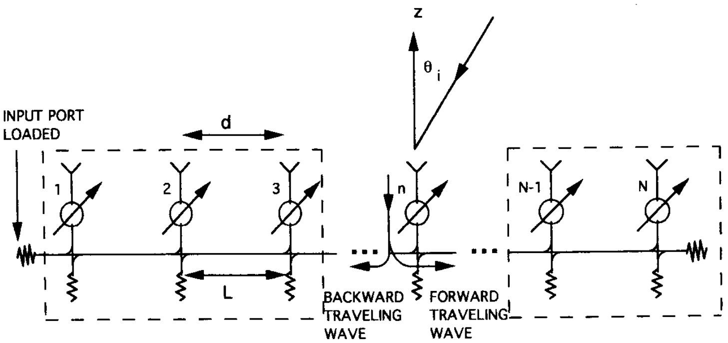

Fig. 3. Forward and backward traveling waves in a series feed network.

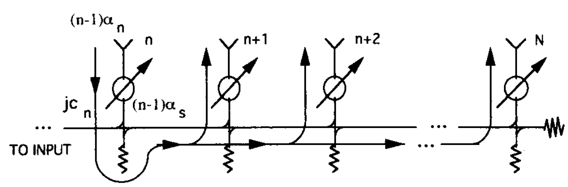

Fig. 4. Forward wave (traveling toward element N).

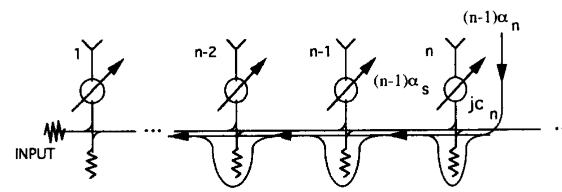

Fig. 5. Backward wave (traveling toward element 1-input).

matched, and to have perfect isolation between the coupled port and through port. The scattering matrix is

$$\boldsymbol{C}_n = \begin{bmatrix} (C_n)_{11} & (C_n)_{12} & (C_n)_{13} & (C_n)_{14} \\ (C_n)_{21} & (C_n)_{22} & (C_n)_{23} & (C_n)_{24} \\ (C_n)_{31} & (C_n)_{32} & (C_n)_{33} & (C_n)_{34} \\ (C_n)_{41} & (C_n)_{42} & (C_n)_{43} & (C_n)_{44} \end{bmatrix} = \begin{bmatrix} 0 & t_n & jc_n & 0 \\ t_n & 0 & 0 & -jc_n \\ jc_n & 0 & 0 & t_n \\ 0 & -jc_n & t_n & 0 \end{bmatrix}. \tag{8}$$

This scattering matrix does not allow for reflections that might originate at the junctions between adjacent couplers. Thus the approximate model only includes reflections from the coupler loads. (Note, however, that reflections at the junctions of the couplers and phase shifters are included through (7).)

To obtain formulas for the feed reflections, E_n, the received incident signal can be decomposed into forward and backward traveling waves on the main line. Fig. 3 shows that a signal received by element n appears as an excitation for the $N-n$ elements toward the load and the $n-1$ elements toward the input. Other scattering components not included in the forward or backward waves are the "self-reflected wave" due to the reflection from the load terminating element n and the "input load reflected wave" due to the reflection from the input load or receiver at the input of the feed. Thus, for each element in the array, four beams are reradiated, and their beamwidths and peak levels depend on the element location in the array. The total scattered field is obtained by the superposition of the forward, backward, self-reflected, and input load reflected waves from all elements.

The formulas for the four waves just described can be obtained by tracing signals through the feed. Let Γ_L be the reflection coefficient of all loads. For an incident signal at element n, a "forward wave" travels toward element N (see Fig. 4) coupling off signals to elements $n+1$ through N as it proceeds. The scattered field can be expressed as[1]

$$\begin{aligned} E_{f_n} \sim & e^{j(n-1)(\alpha_s+\alpha)} jc_n \Gamma_L t_n \{ e^{j\psi_0} jc_{n+1} e^{jn(\alpha_s+\alpha)} \\ & + e^{j2\psi_0} t_{n+1} jc_{n+2} e^{j(n+1)(\alpha_s+\alpha)} + \cdots \\ & + e^{j(N-n)\psi_0} t_{n+1} t_{n+2} \cdots t_{N-1} jc_N \\ & \cdot e^{j(N-1)(\alpha_s+\alpha)}. \end{aligned} \tag{9}$$

The electrical line length between couplers is denoted as ψ_0, and it is equal to k times the physical length of the line ($\psi_0 = kL$). Similar to the forward wave, a "backward wave" travels toward the input (see Fig. 5) radiating reflected signals from elements $n-1$ through 1

$$\begin{aligned} E_{b_n} \sim \Gamma_L e^{j(n-1)(\alpha_s+\alpha)} \Bigg\{ & t_n^2 e^{j(n-1)(\alpha_s+\alpha)} \\ & + jc_n jc_{n-1} t_{n-1} e^{j\psi_0} e^{j(n-2)(\alpha_s+\alpha)} \\ & + jc_n (t_{n-1} e^{j\psi_0}) jc_{n-2} e^{j\psi_0} t_{n-2} e^{j(n-3)(\alpha_s+\alpha)} + \cdots \\ & + jc_{n-1} e^{j\psi_0} \left(\prod_{i=2}^{n-1} t_i e^{j\psi_0} \right) jc_1 t_1 e^{j0(\alpha_s+\alpha)} \Bigg\}. \end{aligned} \tag{10}$$

The self-reflection is due to the load at coupler n, and it is unique in its form

$$E_{\text{self}_n} \sim \Gamma_L t_n^2 e^{j2(n-1)(\alpha_s+\alpha)}. \tag{11}$$

[1] The expressions for the electric field intensity (E) have the leading constants and free space Green's function omitted, because only a ratio is needed in (1).

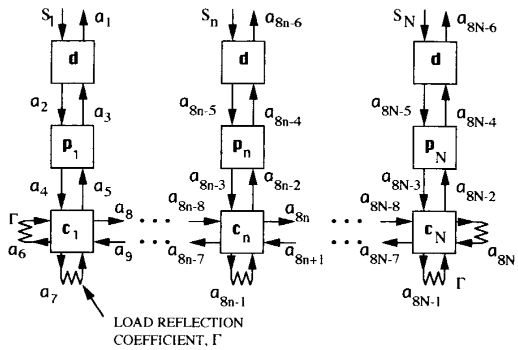

Fig. 6. Scattering matrix representation for the series feed.

Finally, the reflection from the input load is given by

$$E_{\text{in}_n} \sim jc_n e^{j(n-1)(\alpha+\psi_0)} \left[\prod_{m=1}^{n-1} t_m\right] \Gamma_L. \tag{12}$$

The total forward, self, input load, and backward traveling fields from all the elements caused by an incident wave is obtained by summing (9)–(12) over all elements

$$E_{\text{f}} \sim \Gamma_L \sum_{n=1}^{N-1} c_n e^{j(n-1)\zeta} \left\{ \sum_{m=n+1}^{N} c_m e^{j(m-1)\zeta} \cdot \left(\prod_{i=1}^{m-1} t_i e^{j\psi_0} \right) \right\} \tag{13}$$

$$E_{\text{b}} \sim \Gamma_L \sum_{n=1}^{N-1} c_n e^{j(n-1)\zeta} \left\{ \sum_{m=1}^{n-1} c_m e^{j(m-1)\zeta} \cdot \left(\prod_{i=m}^{n-1} t_i e^{j\psi_0} \right) \right\} \tag{14}$$

$$E_{\text{in}} \sim \Gamma_L t_r^2 t_p^2 \left\{ \sum_{n=1}^{N} c_n e^{j(n-1)(\zeta+\psi)} \left(\prod_{m=1}^{n-1} t_m \right) \right\}^2 \tag{15}$$

$$E_{\text{self}} \sim \Gamma_L \sum_{n=1}^{N} t_n^2 e^{j2(n-1)\zeta}. \tag{16}$$

The total scattered field due to the series feed is

$$\begin{aligned} |E_s^s|^2 &= |E_{\text{f}} + E_{\text{b}} + E_{\text{in}} + E_{\text{self}}|^2 \\ &\approx |E_{\text{f}}|^2 + |E_{\text{b}}|^2 + |E_{\text{in}}|^2 + |E_{\text{self}}|^2. \end{aligned} \tag{17}$$

The last approximation is valid if only one term dominates at any particular angle. It is not crucial to the development of the scattering model, but it allows the total RCS to be written as a sum of radar cross sections each associated with an identifiable scattering source. The correct normalization can be obtained by comparing the total scattered field in (17) to the maximum that would be obtained by an array of completely reflecting elements ($= N$). Thus

$$\sigma_s \approx \frac{4\pi A^2 \cos^2\theta}{\lambda^2} t_r^4 t_p^4 \left| \frac{E_s^s}{N} \right|^2. \tag{18}$$

IV. Scattering Matrix Formulation

In the scattering matrix solution, the series feed is represented by an interconnection of two- and four-port devices as shown in Fig. 6. The unknown quantities are the set of signals $\{a_n\}$. A scattering equation can be written at each port, and thus for an N element series fed array, there are $8N$ equations that must be solved simultaneously.

The scattering matrix of the radiating element is

$$d = \begin{bmatrix} d_{11} & d_{12} \\ d_{21} & d_{22} \end{bmatrix} = \begin{bmatrix} r_r & t_r \\ t_r & r_r \end{bmatrix}.$$

For the phase shifter

$$p_n = \begin{bmatrix} (p_n)_{11} & (p_n)_{12} \\ (p_n)_{21} & (p_n)_{22} \end{bmatrix} = \begin{bmatrix} r_p & t_p e^{j(n-1)\alpha_s} \\ t_p e^{j(n-1)\alpha_s} & r_p \end{bmatrix}$$

and the excitations are due to the incident plane wave, $S_n = e^{j(n-1)\alpha}$. Starting with element one, the two scattering equations at the radiating devices are

$$1: \quad a_1 = S_1 d_{11} + a_3 d_{12} \tag{19}$$

$$2: \quad a_2 = S_1 d_{21} + a_3 d_{22} \tag{20}$$

and at the phase shifter ports

$$3: \quad a_3 = a_2 (p_1)_{11} + a_t (p_1)_{12} \tag{21}$$

$$4: \quad a_4 = a_2 (p_1)_{21} + a_5 (p_1)_{22}. \tag{22}$$

Four equations can be written at coupler one (C_1)

$$\begin{aligned} 5: \quad a_6 &= a_6 \Gamma (C_1)_{11} + \Psi a_9 (C_1)_{12} + a_4 (C_1)_{13} \\ &\quad + a_7 \Gamma (C_1)_{14} \end{aligned} \tag{23}$$

$$\begin{aligned} 6: \quad a_8 &= a_6 \Gamma (C_1)_{21} + \Psi a_9 (C_1)_{22} + a_4 (C_1)_{23} \\ &\quad + a_7 \Gamma (C_1)_{24} \end{aligned} \tag{24}$$

$$\begin{aligned} 7: \quad a_5 &= a_6 \Gamma (C_1)_{31} + \Psi a_9 (C_1)_{32} + a_4 (C_1)_{33} \\ &\quad + a_7 \Gamma (C_1)_{34} \end{aligned} \tag{25}$$

$$\begin{aligned} 8: \quad a_7 &= a_6 \Gamma (C_1)_{41} + \Psi a_9 (C_1)_{42} + a_4 (C_1)_{43} \\ &\quad + a_7 \Gamma (C_1)_{44}. \end{aligned} \tag{26}$$

For simplicity, it has been assumed that all loads are identical ($\Gamma_0 = \Gamma_1 = \cdots = \Gamma_N \equiv \Gamma$). Similarly, all inter-coupler line lengths are equal ($\Psi_1 = \Psi_2 = \cdots = \Psi_N \equiv \Psi = e^{j\psi_0}$).

For elements two through N, a pattern repeats. At the radiating element

$$8(n-1)+1: \quad a_{8n-6} = S_n d_{11} + a_{8n-4} d_{12} \tag{27}$$

$$8(n-1)+2: \quad a_{8n-5} = S_n d_{21} + a_{8n-4} d_{22} \tag{28}$$

and the phase shifter

$$8(n-1)+3: \quad a_{8n-4} = a_{8n-5} (p_n)_{11} + a_{8n-2} (p_n)_{12} \tag{29}$$

$$8(n-1)+4: \quad a_{8n-3} = a_{8n-5} (p_n)_{21} + a_{8n-2} (p_n)_{22}. \tag{30}$$

For couplers two through $N-1$

$$8(n-1)+5: \quad a_{8n-7} = \Psi a_{8n-8}(C_n)_{11} + \Psi a_{8n+1}(C_n)_{12} + a_{8n-3}(C_n)_{13} + a_{8n-1}\Gamma(C_n)_{14} \tag{31}$$

$$8(n-1)+6: \quad a_{8n} = \Psi a_{8n-8}(C_n)_{21} + \Psi a_{8n+1}(C_n)_{22} + a_{8n-3}(C_n)_{23} + a_{8n-1}\Gamma(C_n)_{24} \tag{32}$$

$$8(n-1)+7: \quad a_{8n-2} = \Psi a_{8n-8}(C_n)_{31} + \Psi a_{8n+1}(C_n)_{32} + a_{8n-3}(C_n)_{33} + a_{8n-1}\Gamma(C_n)_{34} \tag{33}$$

$$8(n-1)+8: \quad a_{8n-1} = \Psi a_{8n-8}(C_n)_{41} + \Psi a_{8n+1}(C_n)_{42} + a_{8n-3}(C_n)_{43} + a_{8n-1}\Gamma(C_n)_{44}. \tag{34}$$

Finally, coupler N must be treated separately because of the extra load

$$8N-3: \quad a_{8N-7} = \Psi a_{8N-8}(C_N)_{11} + a_{8N}\Gamma(C_N)_{12} + a_{8N-3}(C_N)_{13} + a_{8N-1}\Gamma(C_N)_{14} \tag{35}$$

$$8N-2: \quad a_{8N} = \Psi a_{8N-8}(C_N)_{21} + a_{8N}\Gamma(C_N)_{22} + a_{8N-3}(C_N)_{23} + a_{8N-1}\Gamma(C_N)_{24} \tag{36}$$

$$8N-1: \quad a_{8N-2} = \Psi a_{8N-8}(C_N)_{31} + a_{8N}\Gamma(C_N)_{32} + a_{8N-3}(C_N)_{33} + a_{8N-1}\Gamma(C_N)_{34} \tag{37}$$

$$8N: \quad a_{8N-1} = \Psi a_{8N-8}(C_N)_{41} + a_{8N}\Gamma(C_N)_{42} + a_{8N-3}(C_N)_{43} + a_{8N-1}\Gamma(C_N)_{44}. \tag{38}$$

The above $8N$ equations can be cast into matrix form

$$[S] = [F][a]$$

where the vector $[S]$ contains the excitations $\{S_n\}$ and $[a]$ the unknowns $\{a_n\}$. $[F]$ is a feed scattering matrix obtained from the coefficients of the above equations. The matrix equation is solved to obtain $\{a_n\}$, and the reflection coefficients Γ_n in (5) can be calculated from $a_1, a_{10}, \cdots, a_{8n-6}, \cdots, a_{8N-6}$.

V. Computation and Results

Calculated results are presented for series fed arrays using (5)–(7) and (18). For verification of the approximate method, data are compared with the solution based on scattering matrices. The aperture element is represented by a two-port device with the reflection coefficient r_r allowing direct comparison between the approximate and scattering matrix solutions. This provides a means of evaluating the validity of the assumptions made in deriving the approximate equations.

The array center frequency and that of the illuminating radar are assumed equal (wavelength λ). The coupling coefficients (c_m) are those for uniform array excitation, the element spacing is 0.4λ, and the elements are linearly polarized transverse to the array axis with effective height $\ell = 0.5\lambda$. Several array parameters are varied to study the behavior of RCS. They include the scan angle (θ_s) and the line length between couplers (ψ_0). Figs. 7 and 8 show the difference between the broadside and scanned RCS when $\psi_0 = \pi/4$ rad. It is observed that the highest spike at $\theta = 0$ degrees on both graphs is due to specular scattering from the radiating elements. The spikes at about -20 degrees in Fig. 7 and at 20 degrees in Fig. 8 are due to the reflection from the input load. The spike at -35 degrees in Fig. 8 is due to Bragg diffraction, and the one at 45 degrees is due to the effects of forward and backward waves on the main line scattering retrodirectively. A comparison of the scanned and broadside cases shows the reflections from points behind the phase shifters move toward or away from the specular beam along with the array's radiation beam. The corresponding cases for $\psi_0 = \pi/2$ rad are shown in Figs. 9 and 10.

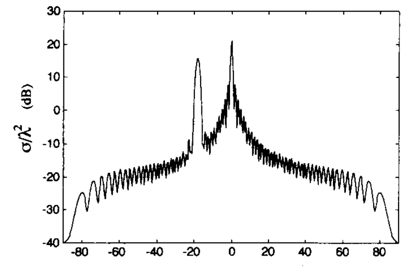

Fig. 7. RCS of series fed array by the approximate method ($\theta_s = 0$ degrees, $\psi_0 = \pi/4$ rad).

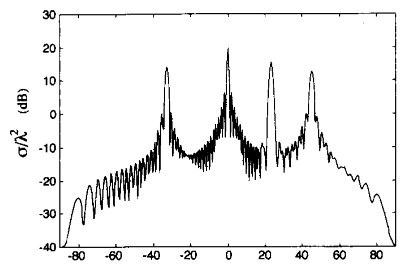

Fig. 8. RCS of series fed array by the approximate method ($\theta_s = 45$ degrees, $\psi_0 = \pi/4$ rad).

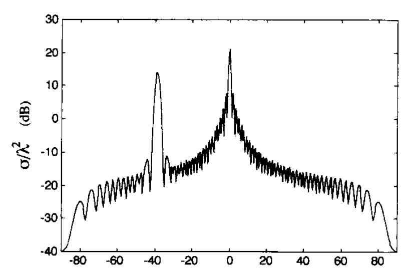

Fig. 9. RCS of series fed array by the approximate method ($\theta_s = 0$ degrees, $\psi_0 = \pi/2$ rad).

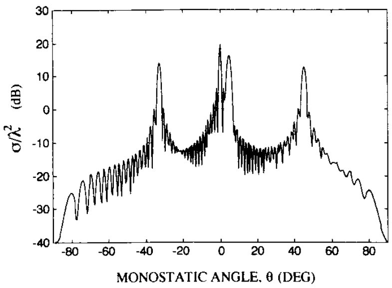

Fig. 10. RCS of series fed array by the approximate method ($\theta_s = 45$ degrees, $\psi_0 = \pi/2$ rad).

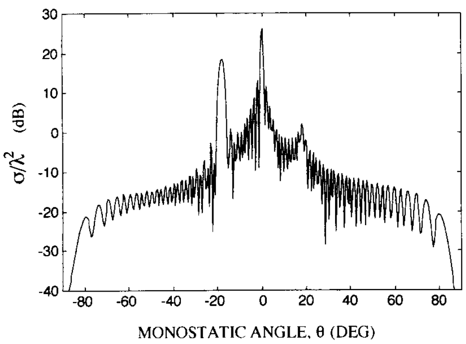

Fig. 11. RCS of series fed array by the scattering matrix method ($\theta_s = 0$ degrees, $\psi_0 = \pi/4$ rad).

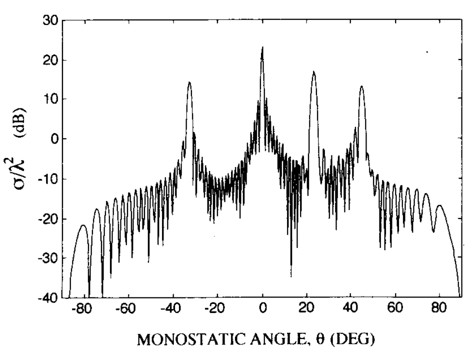

Fig. 12. RCS of series fed array by the scattering matrix method ($\theta_s = 45$ degrees, $\psi_0 = \pi/4$ rad).

In general, the individual spikes can be attributed to specific scattering sources in the antenna. The specular reflection (due to r_r) has its peak at $\theta = 0$ degrees. There is no Bragg diffraction for this term because the element spacing is sufficiently small. Reflections from the input of the phase shifter have a similar behavior as can be seen from (7). Reflected signals from the coupler inputs pass through the phase shifter and therefore scan along with the radiation beam. When the array is scanned, a second lobe originating from r_c appears in the visible region due to Bragg diffraction.

A large lobe also arises due to the reflection from the feed input load. In this case, the array acts as a receive antenna that collects the incident signal. A portion of the signal is reflected

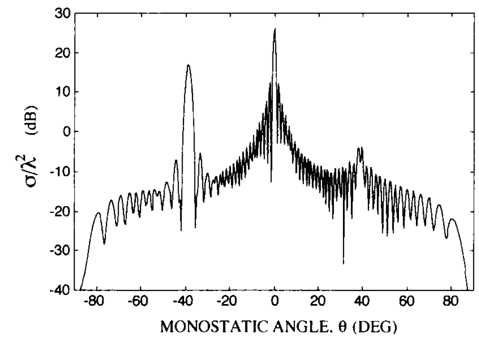

Fig. 13. RCS of series fed array by the scattering matrix method ($\theta_s = 0$ degrees, $\psi_0 = \pi/2$ rad).

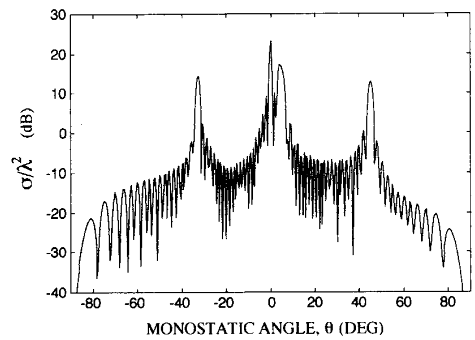

Fig. 14. RCS of series fed array by the scattering matrix method ($\theta_s = 45$ degrees, $\psi_0 = \pi/2$ rad).

at the input terminal and appears just as if a transmit signal has been injected into the antenna. Thus the scattering pattern of this RCS component is the gain pattern squared. It can be seen by comparing Figs. 8 and 10 that the lobe from the input load reflection is determined by ψ_0 as well as θ_s.

The RCS patterns obtained using the scattering matrix method are shown in Figs. 11–14. They correspond to the same cases shown in Figs. 7–10. This solution can be considered rigorous in the sense that all interactions and multiple reflections are included. The agreement between the approximate and the rigorous solutions is excellent in all cases. The approximate formulas correctly predict the locations of all major RCS spikes and their levels to within a couple of dB.

VI. Conclusions

Approximate formulas for the inband RCS of an array with a series feed have been derived. The formulas are based on the hypothesis that an incident wave excites forward and backward traveling waves on the main line. The approximate formulas are in good agreement with results obtained using scattering matrixes, thereby verifying the assumptions made in the approximate solution.

Spikes in the RCS pattern have been identified with specific scattering sources in the array. The parameters affecting the level and location of the lobes have been noted. By properly choosing parameters such as ψ_0 and Γ_L, it is possible to control the spikes to some extent. The RCS data shows, however, that there is no preferred value of ψ_0 that eliminates the input load reflection, although its location can be controlled somewhat by the choice of line length L. Total suppression of the RCS can only be achieved by perfectly matching all of the feed devices which is practically impossible.

The main advantage of the approximate method relative to the scattering matrix method is its speed. The scattering matrix method requires that a matrix equation be solved, and its size increases with the number of array elements. A typical approximate calculation (FORTRAN code for 50 elements and 0.5 degree increments) takes about two minutes on a Sparc 10, whereas the matrix solution runs about two hours. Also, the approximate formulas are easily extended to an arbitrary number of elements. Since both methods assume lossless feed networks and identical reflection coefficients for all similar devices, the actual value of the RCS lobes will be slightly lower than computed here.

REFERENCES

[1] C. G. Montgomery, R. H. Dicke, and E. M. Purcell, *Principles of Microwave Circuits*, MIT Radiation Lab Series. New York: McGraw-Hill, vol. 8, p. 317.

[2] Y. Y. Hu, "Back-scattering cross section of a central-loaded antenna," *IRE Trans. Antennas Propagat.*, vol. AP-6, no. 1, p. 140, Jan. 1985.

[3] D. Midgley, "A theory of receiving aerials applied to the reradiation of an electromagnetic horn," *Proc. IEE*, vol. 108, part B, no. 42, pp. 645–650, Nov. 1961.

[4] N. Williams, "The RCS of antennas—An appraisal," in *Military Microwaves Conf. Proc.*, Brighton, England, June 1986, pp. 505–508.

[5] P. J. Tittensor and M. L. Newton, "Prediction of the radar cross section of an array antenna," in *Proc. 6th Int. Conf. on Antennas Propagat.*, London, England, Apr. 1989, pp. 258–262.

[6] V. Flokas, "Inband scattering from arrays with parallel feed networks," Master's thesis, Naval Postgraduate School, June 1994.

[7] R. C. Hansen, "Relationship between antennas as scatterers and as radiators," *Proc. IEEE*, vol. 77, no. 5, p. 659, May 1989.

[8] D. C. Jenn, "A complete matrix method for antenna analysis," *1988 IEEE AP-S/URSI Symp.*, San Jose, CA, vol. 1, p. 126.

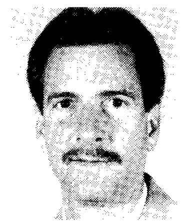

David C. Jenn (S'75–M'82–SM'93) received the B.S. degree in electrical engineering from the University of Wisconsin, Milwaukee, in 1975, the M.S. degree from the Ohio State University, Columbus, under a University Fellowship in 1976, and the Ph.D. degree in electrical engineering from the University of Southern California, Los Angeles, in 1987.

From 1976–1978 he was with McDonnell Douglas Astronautics Co., St. Louis, MO, where he was involved in the design of small arrays and radomes for airborne platforms such as cruise missiles and re-entry vehicles. In 1978 he joined Hughes Aircraft Co., Fullerton, CA, where he concentrated on the design and analysis of high-performance phased array antennas for radar and communication systems. During this period, he completed his Ph.D. as a Hughes Fellow. In the fall of 1990 he joined the Department of Electrical and Computer Engineering at the Naval Postgraduate School, Monterey, CA, as an Associate Professor. His research interests include the application of the method of moments to both array and reflector antenna design, as well as scattering by complex bodies. He is author of the book *Radar and Laser Cross Section Engineering*.

Dr. Jenn is presently serving as Vice-Chairman of the Monterey Bay Subsection. He is also a member of the American Institute of Aeronautics and Astronautics (AIAA), Tau Beta Pi, American Society for Engineering Education (ASEE), and the Applied Computational Electromagnetics Society (ACES).

Seunghoon Lee (S'75–M'82–SM'93) received the B.A. degree in English from the Korean Military Academy in Seoul, Korea, in 1987. He received the M.S. in systems engineering from the Naval Postgraduate School in Monterey, CA, in 1994.

He is currently a Captain in the Republic of Korea Army.